Heliyon 10 (2024) e23672

Contents lists available at ScienceDirect

Heliyon

journal homepage: www.cell.com/heliyon

Identifying potential ferroptosis key genes for diagnosis and treatment of postmenopausal osteoporosis through competitive endogenous RNA network analysis

Chengcheng Huang [a,b,1], Yang Li [c,1], Bo Li [c], Xiujuan Liu [a,b], Dan Luo [a,b], Yuan Liu [a], Mengjuan Wei [b], ZhenGuo Yang [c,**], Yunsheng Xu [c,*]

[a] First Clinical Medical College, Shandong University of Traditional Chinese Medicine, Jinan, Shandong 250000, China
[b] Department of Endocrinology and Metabology, The Affiliated Hospital of Shandong University of Traditional Chinese Medicine, Jinan, Shandong 250000, China
[c] Department of Orthopedic, The Second Affiliated Hospital of Shandong University of Traditional Chinese Medicine, Jinan, Shandong 250000, China

ARTICLE INFO

Keywords:
Postmenopausal osteoporosis
Competitive endogenous RNA
Ferroptosis
Biomarkers
Bioinformatics analysis

ABSTRACT

Objective: Postmenopausal osteoporosis (PMOP) is a common systemic metabolic bone disorder that is owing to the reduced estrogen secretion and imbalance of bone absorption and bone formation in postmenopausal women. Ferroptosis has been identified as a novel modulatory mechanism of osteoporosis. Nevertheless, the particular modulatory mechanism between ferroptosis and PMOP is still unclear. The objective of the current investigation was to detect potential biomarkers connected to ferroptosis in PMOP and discover its probable mechanism through bioinformatics.

Methods: We downloaded PMOP-related microarray datasets from the database of Gene Expression Omnibus (GEO) and obtained the differentially expressed genes (DEGs). Utilizing bioinformatics analysis, the DEGs were intersected with the ferroptosis dataset to obtain ferroptosis-connected mRNAs. Enrichment analysis employing KOBAS 3.0 was conducted to comprehend the biological functions and enrichment pathways of the DEGs. The generation of the protein-protein interaction (PPI) network was conducted with the aim of identifying central genes. Lastly, the coexpression and competitive endogenous RNA (ceRNA) networks were built using Cytoscape. With the help of external datasets GSE56815 to verify the reliability of the hub genes by plotting ROC curves.

Results: We identified 178 DE microRNAs (miRNAs), 138 DE circular RNAs (circRNAs), and 86 ferroptosis-related mRNAs. Enrichment analysis exhibited that mRNAs were primarily connected with the signaling pathways of PI3K/Akt, metabolism, mTOR, FoxO, HIF-1, AMPK, MAPK, ferroptosis, VEGF, and NOD-like receptors. Generation of the PPI network detected eight hub genes. The circRNA/miR-23b-3p/PTEN axis may relieve PMOP by inhibiting ferroptosis through targeting the pathway of PI3K/Akt signaling, which is a vital modulatory pathway for PMOP progression. Moreover, the ROC curves ultimately indicates that the four hub genes have greater diagnostic importance in PMOP samples in contrast to the normal group samples, which may be possible markers for PMOP diagnosis.

* Corresponding author.
** Corresponding author.
E-mail address: 71001953@sdutcm.edu.cn (Y. Xu).
[1] Equal contribution and first authorship: These authors contributed equally to this work and share first authorship.

https://doi.org/10.1016/j.heliyon.2023.e23672
Received 21 February 2023; Received in revised form 24 November 2023; Accepted 9 December 2023
Available online 20 December 2023

Conclusions: Bioinformatics analysis identified four hub genes, namely, PTEN, SIRT1, VEGFA, and KRAS, as potential biomarkers for PMOP diagnosis and management. Moreover, the circRNA/miR-23b-3p/PTEN axis may relieve PMOP by suppressing ferroptosis through targeting the pathway of PI3K/Akt signaling, providing a new avenue to explore the pathogenesis of PMOP.

1. Introduction

Postmenopausal osteoporosis (PMOP) is a common systemic chronic metabolic bone disorder in females in the postmenopausal period. The occurrence of PMOP is mainly due to ovarian atrophy and functional degeneration as well as insufficient estrogen secretion in postmenopausal women, which causes reduced mass of the bone, structural alterations in bone trabeculae, and bone fragility, making bones susceptible to fracture [1]. Osteoporosis (OP) often occurs with several metabolic disorders, such as diabetes, nonalcoholic fatty liver disease (NAFLD), obesity, dyslipidemia, and cardiovascular disease (CVD), in postmenopausal women [2]. This comorbidity poses significant challenges for the management of PMOP. A prior investigation has informed that the frequency of OP in postmenopausal ladies aged above 40 years is 32.5 % in China and gradually increases after the age of 60 years [3]. OP and its complications cause medical and economic burdens to society. At present, the standard method for diagnosis of OP mainly relies on dual-energy X-ray absorptiometry (DXA), but it only provides observations and does not provide analysis of the pathological process, making early diagnosis of OP difficult [4]. More importantly, modern medical treatment for PMOP has many defects, such as diverse side effects, poor tolerance, high cost, poor compliance, bone necrosis, and cancer risk [5]. Therefore, the identification of biomarkers for PMOP has substantial importance in facilitating early identification and management of this condition.

Up to now, the exact PMOP pathogenesis is still unclear. Prior investigations have exhibited that many signaling pathways, like pathways of Wnt/β-catenin signaling, semaphorin 3A (Sema3A)/neuropilin 1 (NRP1)/plexinA1, osteoprotegerin (OPG)/receptor activator of nuclear factor kappa-light-chain-enhancer of activated B cells (NF-κB) ligand (RANKL), oxidative stress, and T cell-mediated inflammatory response, as well as immune cells may participate in the modulation of PMOP, therefore establishing a regulatory network inside the body that eventually disrupts the balance of the remodeling process of the bone [6–9].

Circular RNA (circRNA) is a recently detected kind of non-coding RNA that forms a continuous covalent closed cycle, and it is highly expressed in the eukaryotic transcriptome [10]. Emerging research shows that circRNA can be employed as a treatment target and diagnostic marker of diseases. Moreover, circRNA is also a potential regulator of OP [11]. MicroRNA (miRNA) is a small non-coding RNA that is evolutionarily conserved. Studies have shown that targeting miRNA is expected to become an attractive new method for the management of OP or other orthopedic diseases [12]. The hypothesis of competitive endogenous RNA (ceRNA), as exhibited by Salmena et al. [13], suggests that circRNA acts as a ceRNA and plays a regulatory role by competing with mRNA for miRNA in many diseases, such as PMOP [14]. Ferroptosis is a kind of regulatory cell death that is based on iron and is related to two main biochemical features, namely, lipid peroxidation and iron accumulation [15]. Ferroptosis is connected with the incidence and advancement of several diseases, like cancer, necrotizing inflammatory disease, and CVD [16–18]. A rising number of investigations have stated the connection between ferroptosis and OP, revealing that ferroptosis may be a new treatment target for OP [19,20]. Although there is some evidence that circRNA, miRNA, and ferroptosis have a crucial function in the incidence and OP development, the regulatory impact of these three factors in OP remains to be further investigated, especially during PMOP.

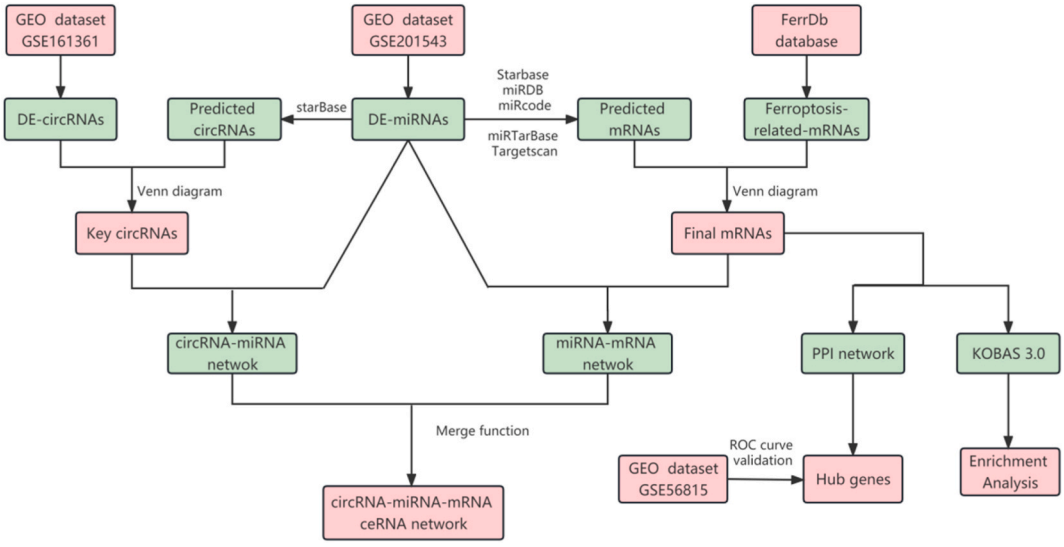

Fig. 1. The detailed workflow of the analysis process.

In the current investigation, we obtained microarray datasets related to PMOP from the database of Gene Expression Omnibus (GEO) and obtained the differentially expressed genes (DEGs). The biological functions and enriched pathways of the DEGs was elucidated utilizing Gene Ontology (GO) and Kyoto Encyclopedia of Genes and Genomes (KEGG) pathway analyses, and we utilized the Search Tool for the Retrieval of Interacting Genes (STRING) database to build a network of protein-protein-interaction (PPI) to detect hub genes. Finally, the coexpression network and ceRNA network were constructed using Cytoscape. Furthermore, we used external datasets GSE56815 to verify the reliability of the hub genes by plotting ROC curves. Using bioinformatics, the current investigation further elucidated the pathogenesis of PMOP, identifying a potential biomarker and modulatory pathway for early PMOP management. The detailed workflow of this investigation is illustrated in a diagram displayed in Fig. 1.

2. Materials and methods

2.1. Microarray data

The GEO online database [21] was searched using the following key words to obtain appropriate gene expression datasets: "postmenopausal osteoporosis" and "*Homo sapiens*". The GSE201543 dataset (containing 6 PMOP samples and 4 normal samples) and the GSE161361 dataset (containing 3 PMOP and 3 healthy specimens) were selected for later examination.

2.2. Data processing and analysis of differential expression

The GPL20712 and GPL28148 platform files were obtained from the GEO database and annotated with probe ID according to the annotation data in the file of the platform. GEO2R (http://www.ncbi.nlm.nih.gov/geo/geo2r/), an interactive webtool that permits users to compare diverse groups of samples across experimental environments in a GEO series, was utilized to identify DEGs. GEO2R online program was used to conduct analysis for the raw submitter-supplied data from the microarrays and to subsequently detect differentially expressed (DE) miRNAs and DEcircRNAs in PMOP. Genes with a log fold change (FC) > 1 or $<$-1 and $P < 0.05$ were reflected as significant DEmiRNAs and DEcircRNAs. It is worth mentioning that logFC >0 represents upregulation, whereas a logFC <0 suggests downregulation. In order to enhance the visualization of DEGs, Hiplot (https://hiplot.com.cn/basic) was employed to build volcano plots and Bioinformatics (http://www.bioinformatics.com.cn) to create heatmaps.

2.3. Screening for key circRNAs

The probable targeting circRNAs of candidate miRNAs was predicted employing the online prediction database, starBase v2.0 (http://starbase.sysu.edu.cn/) [22]. The candidate circRNAs were obtained by intersecting the predicted target circRNAs with DEcircRNAs, which were displayed using a Venn diagram online tool.

2.4. Screening for key mRNAs

Five online mRNA prediction databases, namely, Starbase, miRDB, miRcode, miRTarBase, and Targetscan, were utilized to anticipate target mRNAs of the key genes and to choose mRNAs that were in all databases as the target mRNAs. In addition, the database of FerrDb (http://www.zhounan.org/ferrdb) [23] was utilized to identify genes connected with ferroptosis. The final key mRNAs were obtained through the intersection of predicted mRNAs with ferroptosis-related genes, and they were displayed using a Venn diagram online tool.

2.5. Functional enrichment analysis

A potent online means for functional enrichment analysis KOBAS 3.0 (http://kobas.cbi.pku.edu.cn/genelist/) was employed to conduct GO and KEGG enrichment analyses [24] for further analysis of the DEGs at the level of function. An established P value (Q value) < 0.05 was employed as a filter to screen out significantly enriched functions and pathways. Bioinformatics (http://www.bioinformatics.com.cn) was utilized to visualize the top 10 GO terms, KEGG pathways, and Reactome terms that meet the criterion separately.

2.6. Construction of PPI network

To interpret the molecular pathways of key activities of the cells, the analysis of functional PPI is necessary. In the present study, the STRING database (http://string.embl.de/) [25] and Cytoscape 3.7.2 program [26] were used to build a PPI network featuring the determined mRNAs.The score of reliability minimum interaction was established to the default value of 0.400. Cytoscape software was used to analyze a range of topological features for the nodes in the PPI network, which allowed hub gene detection. The network topology parameters were studied employing the network analyzer plugin in Cytoscape, and significant genes in the network as hub genes were screened utilizing the cytoHubba plugin in Cytoscape [27]. The top ten hub genes were detected by the use of three algorithms, namely, Degree, Maximum Neighborhood Component (MNC), and Maximal Clique Centrality (MCC) [28], and Venn diagram online tool was utilized to display the final hub genes.

2.7. circRNA/miRNA/mRNA ceRNA network construction

The construction of ceRNA network depended on the established interaction connections among circRNAs, miRNAs, and mRNAs. Based on the ceRNA hypothesis, ceRNA expression level should be associated negatively with miRNA expression and positively connected with mRNA expression. Consequently, we included the anticipated associations and the relevant expression data in order to acquire outcomes that are more reliable. In the current investigation, Cytoscape was employed for the creation of circRNA/miRNA and miRNA/mRNA coexpression networks. The merging function in Cytoscape was used to combine the circRNA/miRNA and miRNA/mRNA coexpression networks to obtain the final circRNA/miRNA/mRNA interaction ceRNA regulatory network.

2.8. Hub genes ROC curves

To validate the hub genes reliability, We searched for the keywords "postmenopausal osteoporosis" and "*Homo sapiens*" and found the GSE56815 (comprising 40 high and 40 low hip BMD subjects) from the GEO online database. GEO2R online program was used to analyze the raw submitter-supplied data from the microarrays and to subsequently detect differentially expressed genes in PMOP. The screening criteria for differentially expressed genes are also set to genes with a log fold change (FC) > 1 or <-1 and $P < 0.05$. With the help of Hipplot to generate ROC curves, we analyzed the specific hub gene expression and excavated biomarkers for PMOP diagnosis. Among them, area under the ROC curve (AUC) is a marker that incorporates specificity and sensitivity, representing the internal efficacy of diagnostic tests between 0.5 and 1. A diagnosis is considered to be of higher quality when the AUC value is closer to 1.

3. Results

3.1. DEcircRNAs and DEmiRNAs identification in PMOP

In the current research, the GSE201543 and GSE161361 datasets were normalized to facilitate subsequent data analysis. Depending on the following threshold conditions of p value < 0.05 and logFC >1 or <-1, 178 DEmiRNAs, comprising 126 highly expressed miRNAs and 52 lowly expressed miRNAs, were identified in PMOP samples compared to normal samples. DEGs were visually illustrated employing Heatmap and volcano plot analyses (Fig. 2a and b). In addition, 15,508 DEcircRNAs were significantly and DE between patients with PMOP and controls, including 4643 upregulated and 10,865 downregulated DEcircRNAs. The expression profiles of DEcircRNAs were showed utilizing a heatmap and volcano dot plot (Fig. 3a and b).

3.2. Acquisition of key circRNAs

In the present study, 1292 predicted target circRNAs were identified through starBase v2.0. The key circRNAs were obtained by crossing the predicted target circRNAs with DEcircRNAs obtained in the previous step, and the last key circRNAs were illustrated using

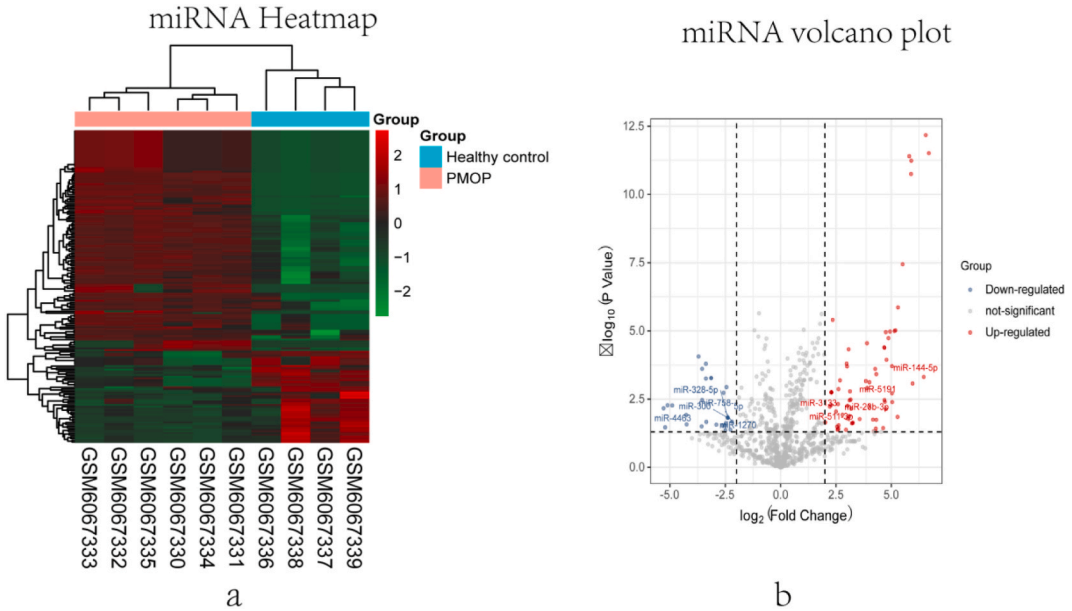

Fig. 2. The heatmap and volcano plot of miRNAs. **a.** miRNA heat map, vertical axis represents sample type, horizontal axis represents gene; **b.** miRNA volcano plot. Red dots represent up-regulated genes, while blue dots represent down-regulated genes. (For interpretation of the references to colour in this figure legend, the reader is referred to the Web version of this article.)

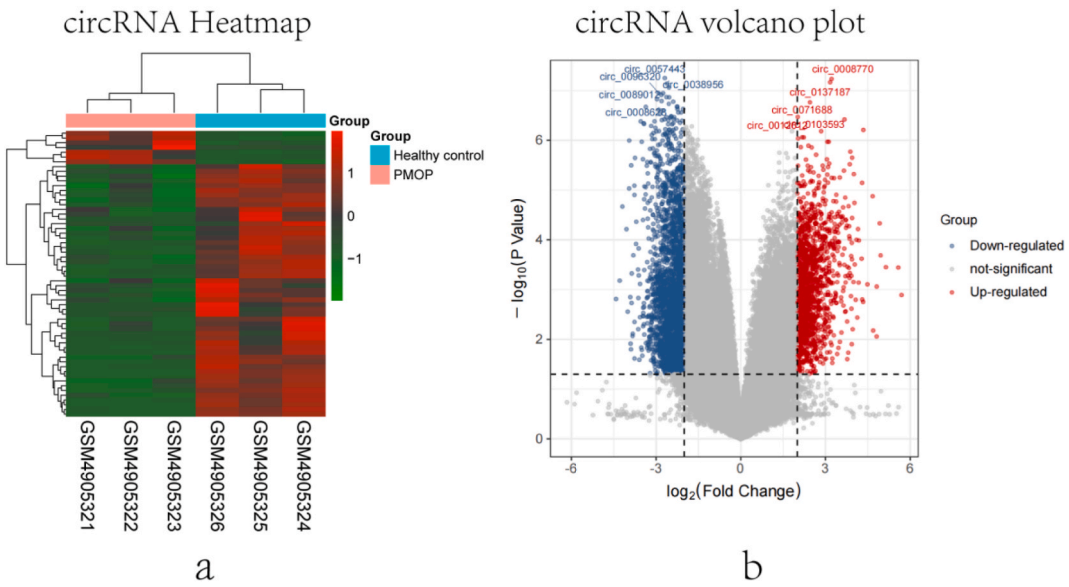

Fig. 3. The heatmap and volcano plot of circRNAs. **a.** cirRNA heat map, vertical axis represents sample type, horizontal axis represents gene; **b.** cirRNA volcano plot. Red dots represent up-regulated genes, while blue dots represent down-regulated genes. (For interpretation of the references to colour in this figure legend, the reader is referred to the Web version of this article.)

the Venn diagram online tool (Supplementary Fig. 1).

3.3. Acquisition of key mRNAs

To obtain the final key mRNAs, we utilized five online databases to anticipate target mRNAs, and their common intersection is shown in Fig. 4a. We next utilized the database of FerrDb to search for ferroptosis-associated genes. The final key mRNAs were acquired through the intersection of predicted mRNAs and genes connected with ferroptosis (Fig. 4b).

3.4. GO and KEGG enrichment analyses of target genes

We used KOBAS 3.0 to conduct GO, KEGG, and Reactome enrichment analyses of the key mRNAs. The major enrichment of key mRNAs was observed in several biological processes, including positive or negative transcription regulation by RNA polymerase II,

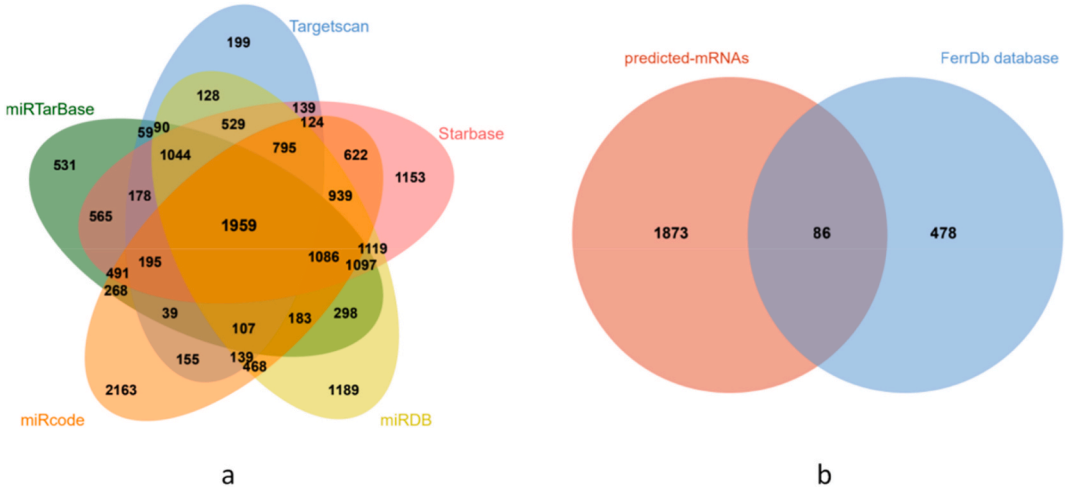

Fig. 4. Acquisition of Key mRNAs. a. The Fig. 4a represents the mRNAs predicted by five online databases. The middle part represents the intersection of the five sets of data. b. The pink part represents the mRNAs predicted by five online databases, the blue part represents the mRNAs obtained from the FerrDb database. The middle part represents the intersection of the two sets of data. (For interpretation of the references to colour in this figure legend, the reader is referred to the Web version of this article.)

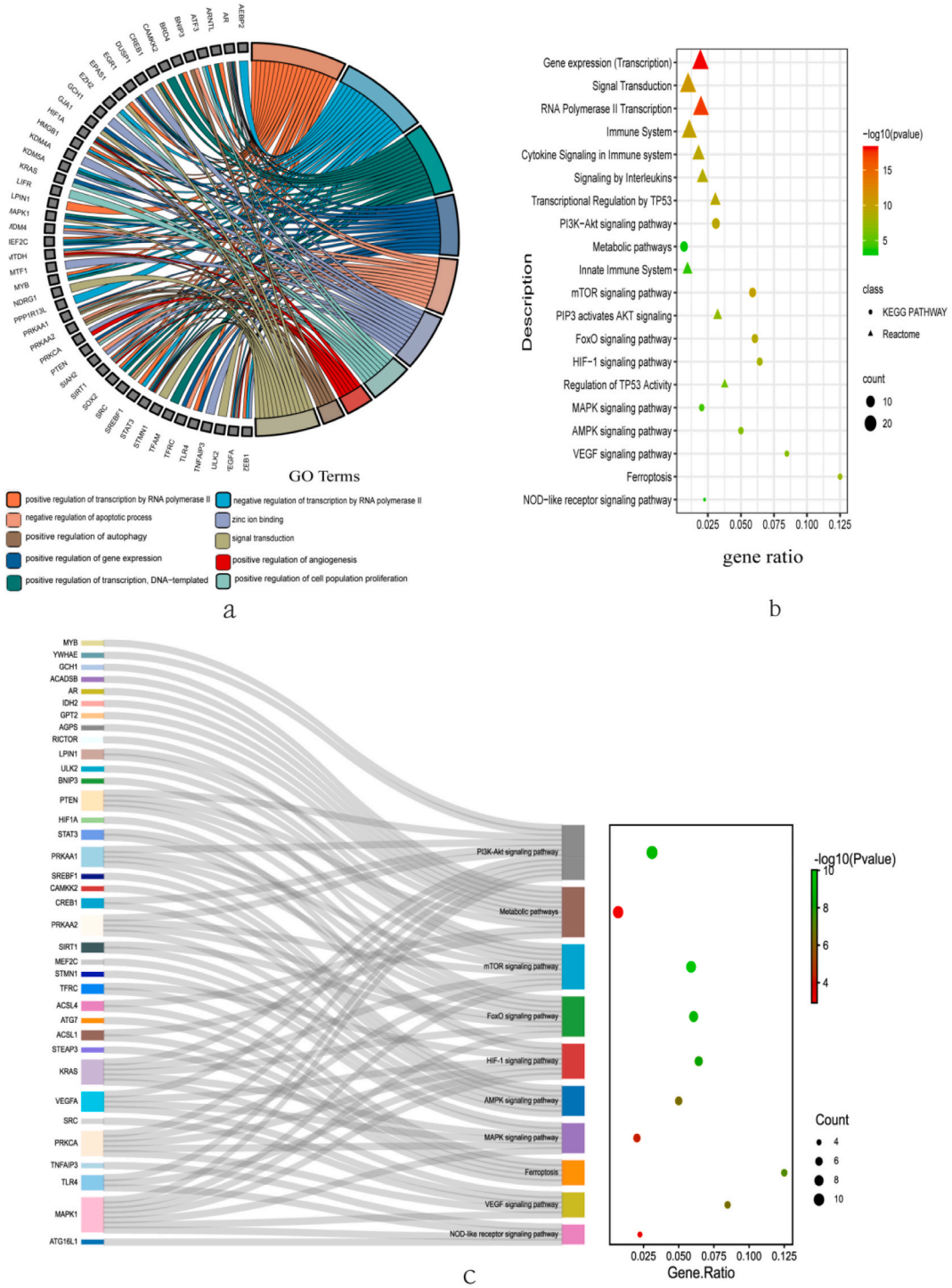

Fig. 5. Enrichment Analysis. **a.** The chord diagram shows that the first 10 biological processes of key mRNAs mainly involves in positive or negative regulation of transcription by RNA polymerase II, positive regulation of gene expression, negative regulation of apoptotic process, positive regulation of cell population proliferation, positive regulation of autophagy, etc. **b.** The bubble plot showing the most enriched KEGG and Reactome terms of key mRNAs. The most significant KEGG pathways involved PI3K-Akt signaling pathway, Metabolic pathways, mTOR signaling pathway, etc. The most significant Reactome terms were Gene expression (Transcription), Signal Transduction, immune system. **c.** The Sankey plot showing the relationship between genes enriched on significant KEGG pathways.

positive gene expression modulation, negative apoptotic process regulation, positive modulation of cell population growth, and positive autophagy regulation. The top ten BPs were selected, and a chord diagram was drawn employing them (Fig. 5a and Table 1). The KEGG enrichment data showed that the mRNAs were mainly connected to pathways of phosphoinositide 3-kinase (PI3K)/Akt signaling, metabolism, mammalian target of rapamycin (mTOR) signaling, forkhead box O (FoxO) signaling, hypoxia-inducible factor 1 (HIF-1) signaling, AMP-activated protein kinase (AMPK) signaling, mitogen-activated protein kinase (MAPK) signaling, ferroptosis, vascular endothelial growth factor (VEGF) signaling, and nucleotide oligomerization domain (NOD)-like receptor signaling. The analysis of Reactome enrichment exhibited that the mRNAs were primarily enriched in gene expression (transcription), signal transduction, immune system, inflammation, and signal. A bubble chart was used to present and analyze the top 10 KEGG pathways and Reactome terms (Fig. 5b and Table 2). Furthermore, a Sankey plot was employed to visually illustrate the connection between enriched genes and significant pathways of KEGG (Fig. 5c).

3.5. PPI network construction and screening of hub genes

The PPI network was built employing the STRING web app and Cytoscape program, and it had 74 nodes and 688 edges, with a 9.29 average degree, as visually represented in Cytoscape (Fig. 6a). The top ten key genes were detected by three procedures, namely, MCC (Fig. 6b), Degree (Fig. 6c), and MNC (Fig. 6d), in the cytoHubba plugin in Cytoscape program, and eight hub genes were obtained through the Venn online tool (Fig. 6e). Phosphatase and tensin homolog (PTEN), signal transducer and activator of transcription 3 (STAT3), HIF1A, silent information regulator 1 (SIRT1), VEGFA, Kirsten rat sarcoma virus (KRAS), enhancer of zeste homolog 2 (EZH2), and SRC were the eight hub genes that identified as the most critical genes within the network of PPI. These genes may have a crucial involvement in PMOP pathogenesis.

3.6. Construction of the circRNA/miRNA/mRNA ceRNA network

To determine the final ceRNA network, a circRNA/miRNA network was created, which included 175 nodes and 397 edges (Fig. 7a). A miRNA/mRNA network was built, which included 213 nodes and 1254 edges (Fig. 7b). The merge function in Cytoscape program was employed to combine circRNA/miRNA network and miRNA/mRNA network to obtain the final ceRNA network, which was composed of 251 nodes and 1228 edges (Fig. 8a).

The ceRNA hypothesis [13] describes a complicated posttranscriptional regulatory mechanism in cells, including lncRNAs, circRNAs, and other RNAs, which function as sponges to jointly compete for the binding sites of miRNAs to reduce the expression of miRNAs, thus interfering with the miRNA-induced inhibition of downstream target genes. Previous studies have shown that functional interaction was observed between multiple miRNAs and PTEN, which suppresses its expression, thereby participating in various disease pathogenesis, like cancer, cerebral ischemic stroke, OP, acute injury of the kidney, hepatic fibrosis, pulmonary hypertension, myocardial infarction, infertility, osteoarthritis, acute pancreatic inflammation, and atherosclerosis [29]. Compared to healthy individuals, patients with OP have lower expression levels of PTEN [30]. miRNA/PTEN axes have a significant function in human disease pathogenesis, and treatment targets of these axes will have advantageous impacts on various diseases. Therefore, we selected PTEN to establish a miRNA/PTEN network for further analysis (Fig. 8b). Depending on the theory of the ceRNA hypothesis, miR-23b-3p is significantly upregulated in individuals with PMOP [31], which was in line with the present outcomes. In addition, a previous investigation has reported that miR-23b-3p enhances osteoclasts differentiation via the PTEN cascade, and the direct target of miR-23b–3p in osteoclasts is PTEN [32]. Therefore, in accordance with the modulatory connection among circRNAs, miRNAs, and mRNAs, a hub ceRNA network was built for further analysis utilizing hsa-miR-23b-3p (Fig. 8c).

3.7. ROC curve of ferroptosis-connected hub genes in PMOP

To validate the hub genes' reliability, increase the local specificity of the hub genes, and identify potential biomarkers throughout the entire process of disease occurrence and development in PMOP, the ROC curves of the eight hub genes related to ferroptosis in PMOP were validated using the GSE56815 datasets. The results are shown in Fig. 9. The diagnostic importance of these hub genes in PMOP samples is as follows: SIRT1(AUC:0.790), VEGFA (AUC: 0.767), KRAS (AUC: 0.762), PTEN (AUC: 0.642). Overall, out of these

Table 1
Deatelis of top 10 GO terms.

Term	Description	Count	*P*-Value
GO:0045,944	positive regulation of transcription by RNA polymerase II	19	7.99E-12
GO:0000122	negative regulation of transcription by RNA polymerase II	18	3.42E-13
GO:0045,893	positive regulation of transcription, DNA-templated	15	1.89E-12
GO:0010,628	positive regulation of gene expression	13	5.17E-12
GO:0007165	signal transduction	13	3.60E-07
GO:0043,066	negative regulation of apoptotic process	12	9.97E-10
GO:0008270	zinc ion binding	12	2.71E-07
GO:0008284	positive regulation of cell population proliferation	9	1.83E-06
GO:0045,766	positive regulation of angiogenesis	6	5.98E-07
GO:0010,508	positive regulation of autophagy	5	2.83E-07

Table 2
Deatelis of top 10 KEGG pathway.

Pathyway ID	Term	Count	*P*-Value	Genes
hsa 04151	PI3K-Akt signaling pathway	11	4.97E-10	YWHAE, PRKCA,PRKAA2,PRKAA1,PTEN, MAPK1,VEGFA, CREB1,TLR4,MYB, KRAS
hsa 01100	Metabolic pathways	10	0.001208	AGPS, LPIN1,GPT2,IDH2,ACSL1,ACSL4,PTEN,AR,ACADSB,GCH1
hsa 04150	mTOR signaling pathway	9	9.56E-11	ULK2,LPIN1,PRKCA, PRKAA2,PRKAA1,PTEN, MAPK1,RICTOR, KRAS
hsa 04068	FoxO signaling pathway	8	8.84E-10	SIRT1,STAT3,PRKAA2,PRKAA1,PTEN, MAPK1,KRAS, BNIP3
hsa 04066	HIF-1 signaling pathway	7	7.16E-09	STAT3,TFRC, PRKCA,HIF1A,MAPK1,VEGFA,TLR4
hsa 04152	AMPK signaling pathway	6	3.66E-07	SIRT1,PRKAA2,CREB1,CAMKK2,SREBF1,PRKAA1
hsa 04010	MAPK signaling pathway	6	5.38E-05	STMN1,PRKCA,MEF2C,MAPK1,VEGFA, KRAS
hsa 04216	Ferroptosis	5	5.07E-08	STEAP3,ACSL1,ATG7,ACSL4,TFRC
hsa 04370	VEGF signaling pathway	5	3.06E-07	PRKCA,SRC,MAPK1,VEGFA, KRAS
hsa 04621	NOD-like receptor signaling pathway	4	0.000701	ATG16L1,MAPK1,TLR4,TNFAIP3

eight hub genes, four hub genes have good diagnostic performance in PMOP and are expected to become potential biomarkers related to ferroptosis in PMOP.

4. Discussion

PMOP is categorized by decreased mass of bone and degeneration of bone microstructure as well as by increased susceptibility to brittle fracture, resulting in disability and mortality [33]. Due to the rapid aging of the global people, the number of subjects with OP is growing, especially among postmenopausal women, resulting in challenges to individual families and health care [34]. Therefore, early molecular diagnosis and intervention for postmenopausal OP patients has far-reaching clinical significance.

In this investigation, KEGG enrichment analysis showed that mRNAs were primarily connected with the pathways of PI3K/Akt signaling, metabolism, mTOR signaling, FoxO signaling, HIF-1 signaling, AMPK signaling, MAPK signaling, ferroptosis, VEGF signaling, and NOD-like receptor signaling. Eight hub genes, namely, PTEN, HIF1A, SIRT1, STAT3, VEGFA, KRAS, EZH2, and SRC, were obtained through the PPI network. In addition, the ROC curve results also show that compared with the normal group samples, among these eight hub genes, the four hub genes namely SIRT1, VEGFA, KRAS, and PTEN have higher diagnostic value in PMOP samples, and are expected to become potential biomarkers for ferroptosis related diagnosis in PMOP. However, although the other four genes did not exhibit good diagnostic value, this may be related to the small sample size. In the future, we will conduct basic experiments to further verify our presumption. PTEN is a dual-function phosphatase that exhibits both protein and lipid phosphatase activities. It serves as a cancer inhibitor and has a vital role in the regulation of metabolism [35]. Chai et al. reported that the modulation of osteoclast differentiation is mediated by miR-23b-3p, which exerts its effects via targeting PTEN through the pathway of PI3K/Akt [32], suggesting that PTEN has a vital function in bone homeostasis. PTEN has been recognized as a significant regulatory component in the differentiation of osteoblast and apoptosis; mir-708 suppresses MC3T3-E1 osteoblasts against apoptosis induced by H2O2 via directly targeting PTEN [36]. Research reports that lncRNA-ORLNC1 inhibits the differentiation of osteogen and enhances adipogenic differentiation of BMSCs in vitro; in addition, it efficiently inhibits the accelerating effect of miR-296 on the differentiation of osteoblasts by targeting PTEN. The lncRNA-ORLNC1-miR-296-PTEN axis may be a vital regulatory factor for the transition connected with osteoporosis between osteogenesis and adipogenesis in BMSC and may be a possible treatment target for improving osteoporotic bone loss [37]. SIRT1 is a significant regulator of cell survival and lifespan, and it has great potential in predicting and managing diseases connected with bone, such as OP and osteonecrosis, indicating that SIRT1 may be a promising bone homeostasis modulator [38]. It has been reported that resveratrol treatment enhances mitochondrial autophagy by the mediation of both pathways of SIRT1 and PI3K/Akt/mTOR signaling, thus protecting osteoblasts in OP rats [39]. Moreover, a previous study has demonstrated that vitamin K2 ameliorates osteoporosis related to type 2 diabetes through AMPK/SIRT1 signaling pathway activation to suppress ferroptosis [40]. Vascular endothelial growth factor (VEGF) is a factor of endothelial cell survival and is necessary for the efficient connection between angiogenesis and osteogenesis. A previous study has reported that miR-16–5p inhibits osteogenesis by suppressing VEGFA expression, which is a PMOP-favorable treatment target [41]. Wang et al. reported that Dexmedetomidine can enhance VEGFA by suppressing miR-361–5p, thereby promoting osteogenic angiogenesis and providing potential PMOP curative targets [42]. Studies have shown that VEGFA is a miR-10a-3p target gene. The overexpression of lncRNA GAS5 increases angiogenesis by suppressing miR-10a-3p and promoting the VEGFA expression, which provides a novel target for medical therapy of OP [43]. KRAS is the most common protein of the RAS gene family, and it plays a vital function in cell proliferation and cell division as well as contributes to the development of many cancers, like bone [44], pancreatic, lung, and colon cancers [45]. Hu et al. demonstrated that KRAS expression level is significantly reduced in OP-bone marrow stromal cells (BMSCs); in addition, they reported that miR-210–3p suppresses the osteogenic differentiation process of normal BMSCs by targeting KRAS and inhibiting MAPK signal transduction, but KRAS overexpression reverses the suppression of miR-210–3p overexpression [46].

Because ferroptosis plays a key role in PMOP, we identified genes related to PMOP and ferroptosis, which may help to identify potential therapeutic targets or offer a theoretical foundation for understanding the molecular pathology of PMOP. We generated a ceRNA network using Cytoscape software and further constructed the circRNA/miR-23b-3p/PTEN network depending on the theory of ceRNA and numerous previous studies. To date, there are few studies on the expression profile and circRNAs modulatory mechanisms

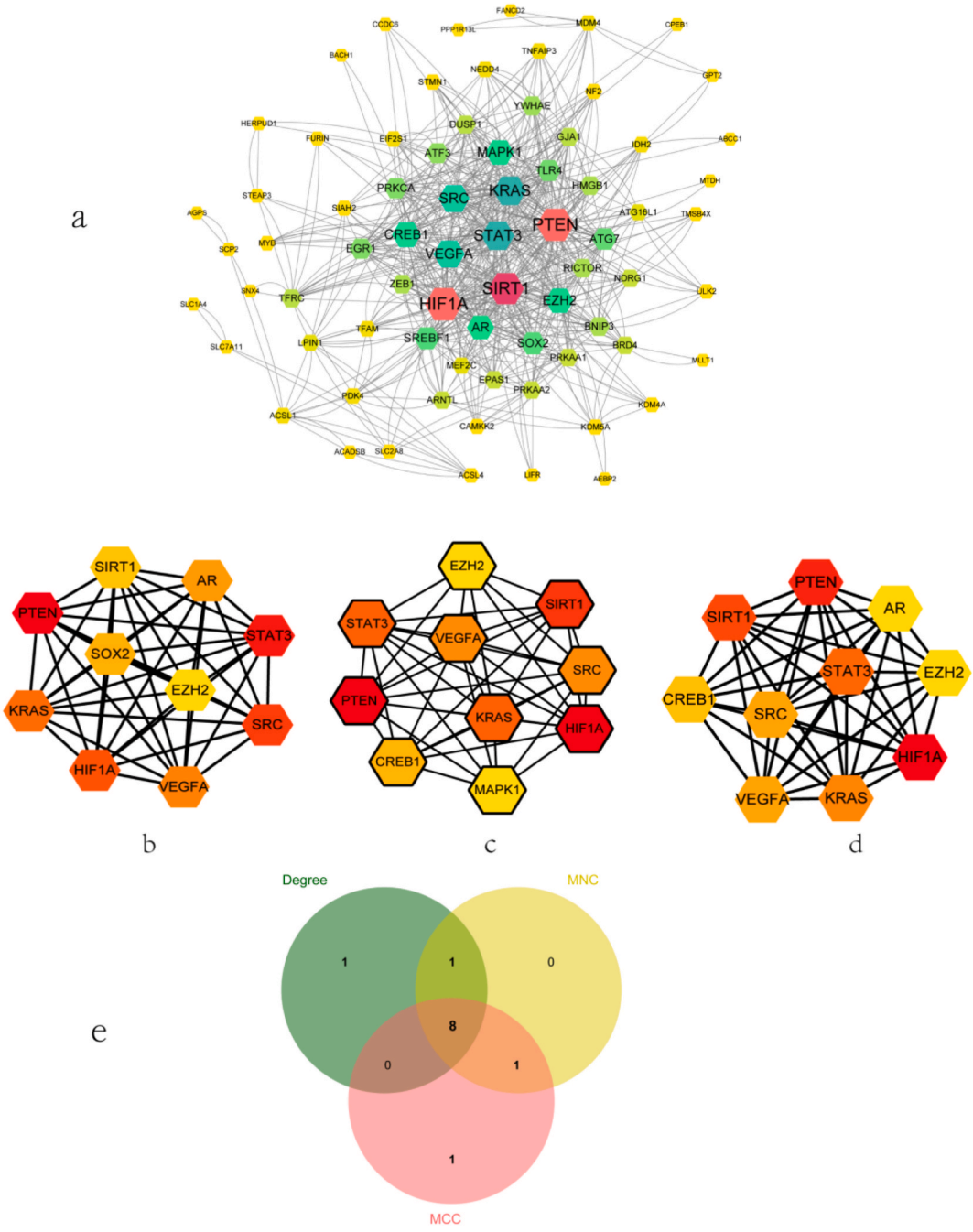

Fig. 6. PPI network and hub genes identification. **a.** The PPI network was comprised of 74 nodes and 688 edges. Each node represents a protein, while each edge represents one protein–protein association. The larger the degree value, the larger the shape size. **b-d.** The hub genes were identified using three models (MCC, Degree and MNC) with the Cytoscape plug-in cytoHubba. **e.** The Venn diagram was used to identify the eight hub genes in PMOP.

in PMOP. Therefore, it is imperative to study the relationship between circRNA expression and the development of PMOP. KEGG enrichment analysis suggested that the pathway of PI3K/Akt signaling had the highest level of enrichment among the mRNAs associated with ferroptosis. It has been informed that the PTEN/PI3K/Akt signal pathway regulates the signal transduction of various biological processes like proliferation, growth, and cell apoptosis [47]. Based on prior studies [48,49], the pathway of PI3K is strictly connected with ferroptosis, cell growth, and osteoporosis, and activation of this pathway protects cells from ferroptosis, thus alleviating osteoporosis. The circRNA/miR-23b-3p/PTEN axis may relieve PMOP by suppressing ferroptosis by targeting the pathway of PI3K/Akt signaling, which may be a vital modulatory pathway for progression of PMOP.

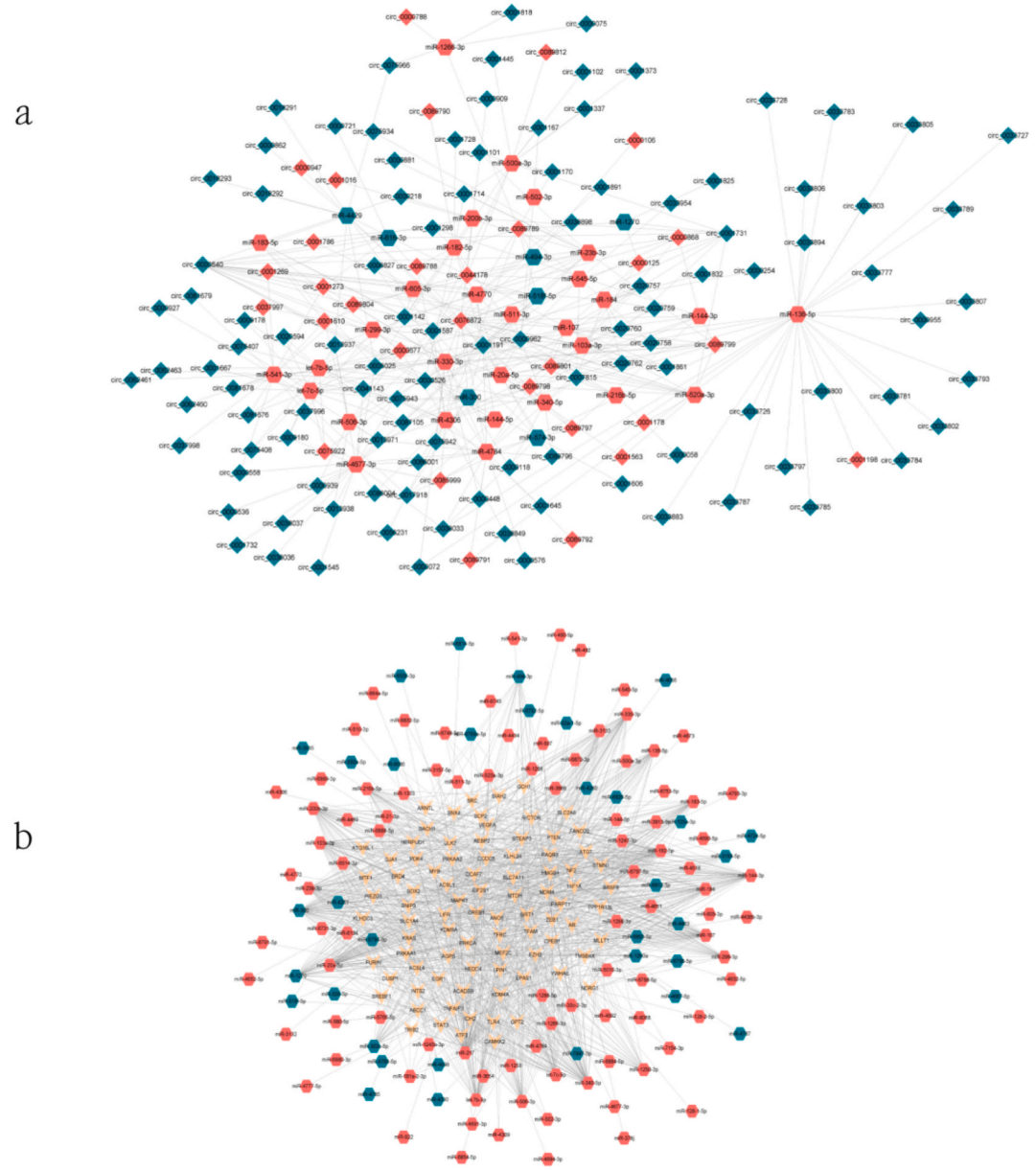

Fig. 7. The circRNA-miRNA network and miRNA-mRNA network construction. **a.** The circRNA-miRNA co-expressed network was constructed by Cytoscape which including 175 nodes and 397 edges. One node represents a circRNA or miRNA, while one edge represents one interaction of circRNA and miRNA. The diamond represents circRNA, while the hexagon represents miRNA (the red figure represents the up-regulated gene, and the green figure represents the down-regulated gene). **b.** The miRNA-mRNA co-expressed network was constructed by Cytoscape which including 213 nodes and 1254 edges. One node represents a miRNA or mRNA, while one edge represents one interaction of miRNA and mRNA. The hexagon represents miRNA, while the inverted triangle represents mRNA (the red figure represents the up-regulated gene, and the green figure represents the down-regulated gene). (For interpretation of the references to colour in this figure legend, the reader is referred to the Web version of this article.)

5. Conclusion

In the current investigation, we detected four specifically expressed ferroptosis-related hub genes, namely, PTEN, SIRT1, VEGFA, and KRAS, which may be potential markers for PMOP diagnosis and tharapy. The circRNA/miR-23b-3p/PTEN axis may relieve PMOP by inhibiting ferroptosis though targeting PI3K/Akt signaling pathway, thus providing a basis for further exploring the potential therapeutic targets and regulatory mechanisms of PMOP as well as a new therapeutic strategy. Due to the inherent limitations of bioinformatics, including untimely database updates, in addition to the relative small sample size in the present study, further validation using larger sample sizes, basic experiments, and prospective studies is required in the future.

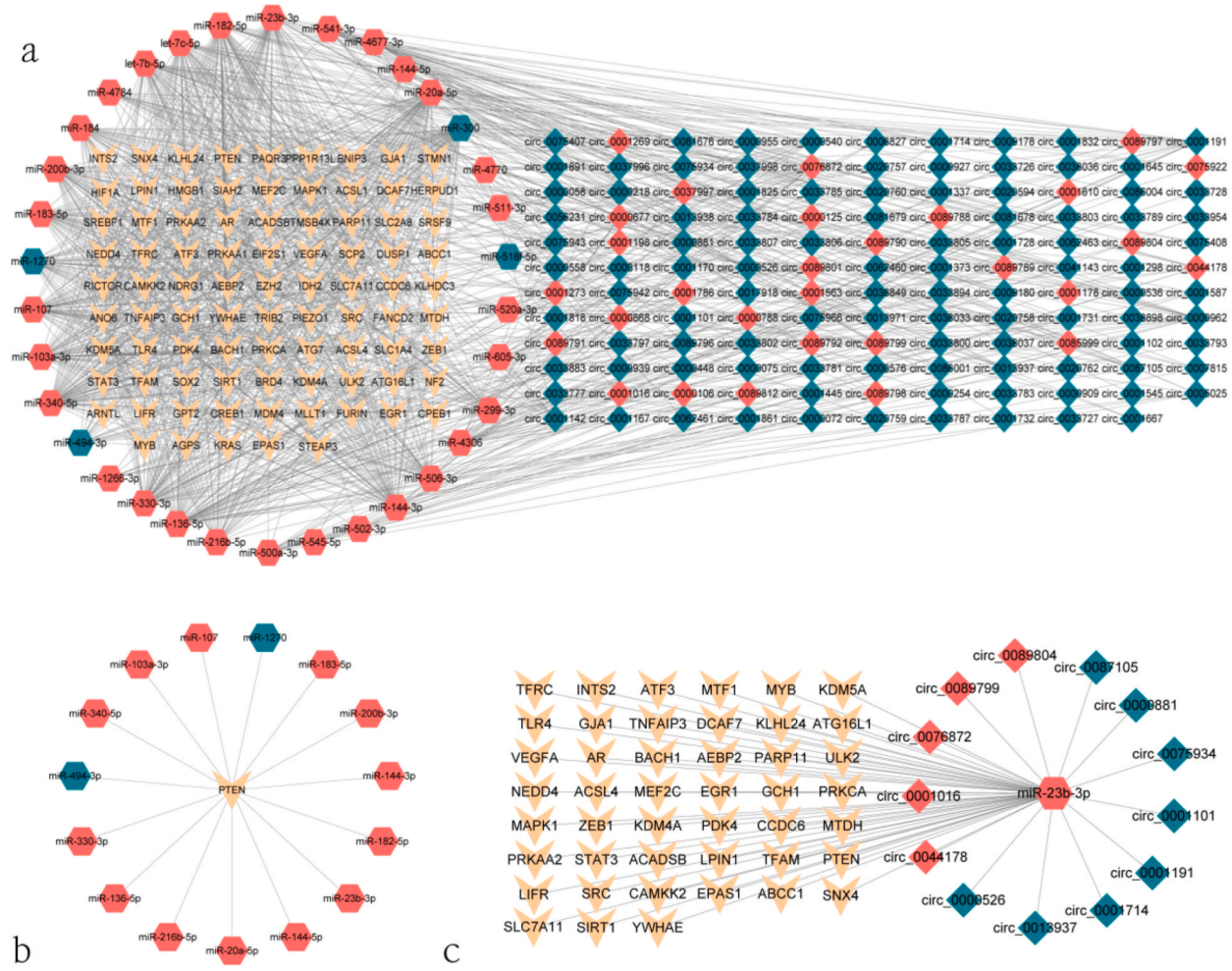

Fig. 8. The ceRNA network and its potential RNA regulation pathway. **a.** The ceRNA regulatory network (The hexagon represents miRNA, the diamond represents circRNA, and the inverted triangle represents mRNA). **b.** The miRNAs-PTEN network. **C.** The circRNAs-miR-23b-3p-mRNAs ceRNA network.

Funding

None.

Data availability statement

The data related to our research has been stored in a publicly available repository. The GSE datasets are accessible in the database of GEO (https://www.ncbi.nlm.nih.gov/geo/) with the following data accession identifier(s):GSE161361 and GSE201543.

CRediT authorship contribution statement

Chengcheng Huang: Writing – original draft. **Yang Li:** Writing – original draft, Data curation, Conceptualization. **Bo Li:** Validation, Software. **Xiujuan Liu:** Validation, Software. **Dan Luo:** Visualization. **Yuan Liu:** Visualization. **Mengjuan Wei:** Validation. **ZhenGuo Yang:** Writing – review & editing. **Yunsheng Xu:** Writing – review & editing, Conceptualization.

Declaration of competing interest

The authors declare that they have no known competing financial interests or personal relationships that could have appeared to influence the work reported in this paper.

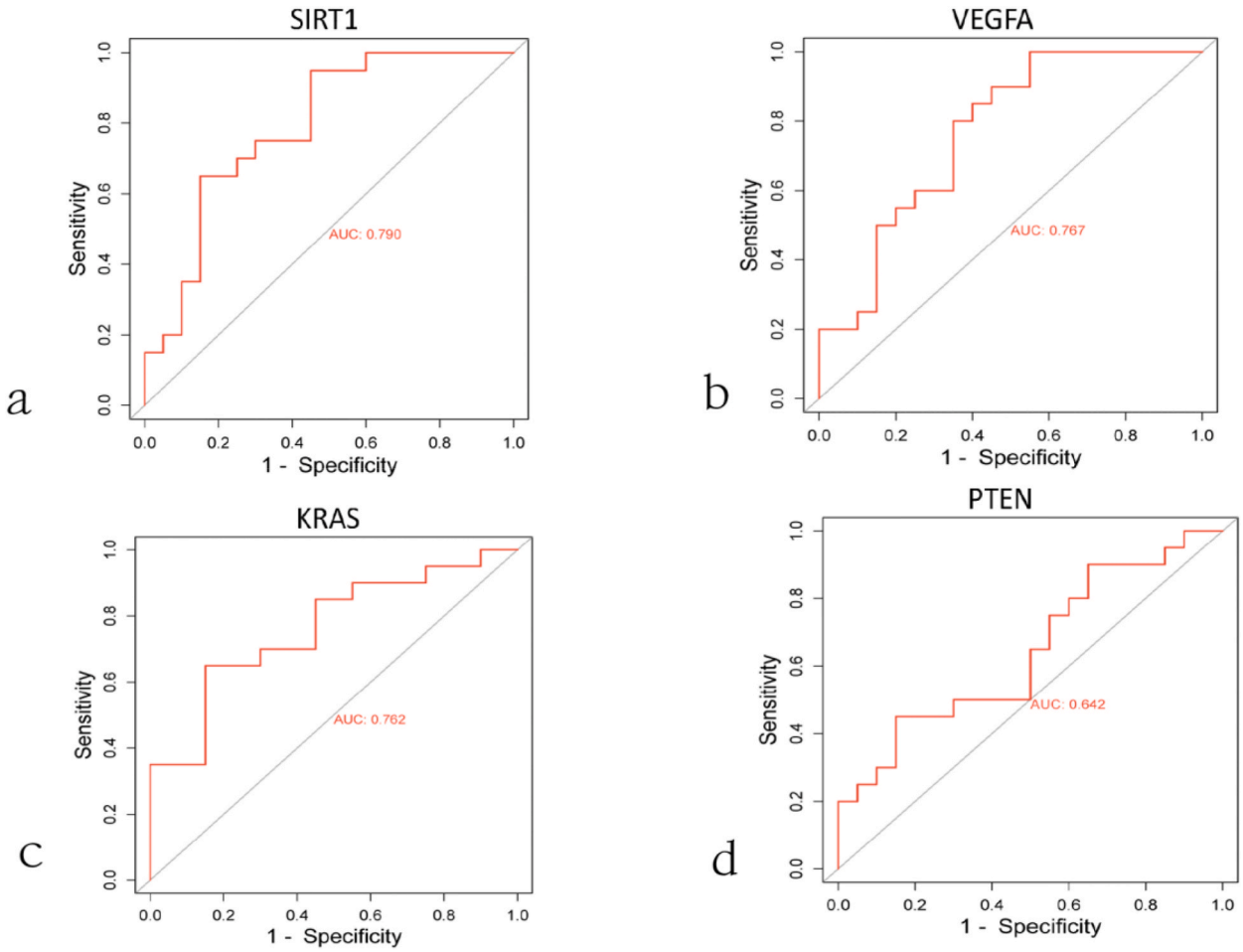

Fig. 9. ROC curves of ferroptosis-related hub genes in PMOP. **a.** Sensitivity of SIRT1 in the diagnosis of PMOP. **b.** Sensitivity of VEGFA in the diagnosis of PMOP. **c.** Sensitivity of KRAS in the diagnosis of PMOP. **d**. Sensitivity of PTEN in the diagnosis of PMOP.

Acknowledgments

None.

Appendix A. Supplementary data

Supplementary data to this article can be found online at https://doi.org/10.1016/j.heliyon.2023.e23672.

References

[1] Y. Deng, W. He, H. Cai, J. Jiang, Y. Yang, Y. Dan, H. Luo, Y. Du, L. Chen, B. He, Analysis and validation of hub genes in blood monocytes of postmenopausal osteoporosis patients, Front. Endocrinol. 12 (2021), 815245, https://doi.org/10.3389/fendo.2021.815245.
[2] S.A. Polyzos, A.D. Anastasilakis, Z.A. Efstathiadou, M.P. Yavropoulou, P. Makras, Postmenopausal osteoporosis coexisting with other metabolic diseases: treatment considerations, Maturitas 147 (2021) 19–25, https://doi.org/10.1016/j.maturitas.2021.02.007.
[3] S. Tang, X. Yin, W. Yu, L. Cui, Z. Li, L. Cui, L. Wang, W. Xia, [Prevalence of osteoporosis and related factors in postmenopausal women aged 40 and above in China], Zhonghua Liuxingbingxue Zazhi 43 (4) (2022) 509–516, https://doi.org/10.3760/cma.j.cn112338-20210826-00680.
[4] J. Kou, C. He, L. Cui, Z. Zhang, W. Wang, L. Tan, D. Liu, W. Zheng, W. Gu, N. Xia, Discovery of potential biomarkers for postmenopausal osteoporosis based on untargeted GC/LC-MS, Front. Endocrinol. 13 (2022), 849076, https://doi.org/10.3389/fendo.2022.849076.
[5] P. Sun, C. Zhang, Y. Huang, J. Yang, F. Zhou, J. Zeng, Y. Lin, Jiangu granule ameliorated OVX rats bone loss by modulating gut microbiota-SCFAs-Treg/Th17 axis, Biomed. Pharmacother. 150 (2022), 112975, https://doi.org/10.1016/j.biopha.2022.112975.
[6] D. Wu, A. Cline-Smith, E. Shashkova, A. Perla, A. Katyal, R. Aurora, T-cell mediated inflammation in postmenopausal osteoporosis, Front. Immunol. 12 (2021), 687551, https://doi.org/10.3389/fimmu.2021.687551.
[7] V. Fischer, M. Haffner-Luntzer, Interaction between bone and immune cells: implications for postmenopausal osteoporosis, Semin. Cell Dev. Biol. 123 (2022) 14–21, https://doi.org/10.1016/j.semcdb.2021.05.014.

[8] G. Shen, H. Ren, Q. Shang, W. Zhao, Z. Zhang, X. Yu, K. Tang, J. Tang, Z. Yang, D. Liang, et al., Foxf1 knockdown promotes BMSC osteogenesis in part by activating the Wnt/β-catenin signalling pathway and prevents ovariectomy-induced bone loss, EBioMedicine 52 (2020), 102626, https://doi.org/10.1016/j.ebiom.2020.102626.

[9] Y.-Q. Liu, X.-F. Han, J.-X. Bo, H.-P. Ma, Wedelolactone enhances osteoblastogenesis but inhibits osteoclastogenesis through Sema3A/NRP1/PlexinA1 pathway, Front. Pharmacol. 7 (2016) 375.

[10] T.B. Hansen, T.I. Jensen, B.H. Clausen, J.B. Bramsen, B. Finsen, C.K. Damgaard, J. Kjems, Natural RNA circles function as efficient microRNA sponges, Nature 495 (7441) (2013) 384–388, https://doi.org/10.1038/nature11993.

[11] X. Pan, X. Cen, B. Zhang, F. Pei, W. Huang, X. Huang, Z. Zhao, Circular RNAs as potential regulators in bone remodeling: a narrative review, Ann. Transl. Med. 9 (19) (2021) 1505, https://doi.org/10.21037/atm-21-2114.

[12] L. Gennari, S. Bianciardi, D. Merlotti, MicroRNAs in bone diseases, Osteoporos. Int. 28 (4) (2017) 1191–1213, https://doi.org/10.1007/s00198-016-3847-5.

[13] L. Salmena, L. Poliseno, Y. Tay, L. Kats, P.P. Pandolfi, A ceRNA hypothesis: the Rosetta Stone of a hidden RNA language? Cell 146 (3) (2011) 353–358, https://doi.org/10.1016/j.cell.2011.07.014.

[14] H. Wang, K. Zhou, F. Xiao, Z. Huang, J. Xu, G. Chen, Y. Liu, H. Gu, Identification of circRNA-associated ceRNA network in BMSCs of OVX models for postmenopausal osteoporosis, Sci. Rep. 10 (1) (2020), 10896, https://doi.org/10.1038/s41598-020-67750-8.

[15] D. Tang, X. Chen, R. Kang, G. Kroemer, Ferroptosis: molecular mechanisms and health implications, Cell Res. 31 (2) (2021) 107–125, https://doi.org/10.1038/s41422-020-00441-1.

[16] J. Zhao, Y. Zhao, X. Ma, B. Zhang, H. Feng, Targeting ferroptosis in osteosarcoma, J Bone Oncol 30 (2021), 100380, https://doi.org/10.1016/j.jbo.2021.100380.

[17] J. Li, Y. Yao, Y. Tian, Ferroptosis: a trigger of proinflammatory state progression to immunogenicity in necroinflammatory disease, Front. Immunol. 12 (2021), 701163, https://doi.org/10.3389/fimmu.2021.701163.

[18] H. Hu, Y. Chen, L. Jing, C. Zhai, L. Shen, The link between ferroptosis and cardiovascular diseases: a novel target for treatment, Front Cardiovasc Med 8 (2021), 710963, https://doi.org/10.3389/fcvm.2021.710963.

[19] Z. Gao, Z. Chen, Z. Xiong, X. Liu, Ferroptosis - a new target of osteoporosis, Exp. Gerontol. 165 (2022), 111836, https://doi.org/10.1016/j.exger.2022.111836.

[20] Y. Lin, X. Shen, Y. Ke, C. Lan, X. Chen, B. Liang, Y. Zhang, S. Yan, Activation of osteoblast ferroptosis via the METTL3/ASK1-p38 signaling pathway in high glucose and high fat (HGHF)-induced diabetic bone loss, Faseb. J. 36 (3) (2022), e22147, https://doi.org/10.1096/fj.202101610R.

[21] T. Barrett, S.E. Wilhite, P. Ledoux, C. Evangelista, I.F. Kim, M. Tomashevsky, K.A. Marshall, K.H. Phillippy, P.M. Sherman, M. Holko, et al., NCBI GEO: archive for functional genomics data sets–update, Nucleic Acids Res. 41 (Database issue) (2013) D991–D995, https://doi.org/10.1093/nar/gks1193.

[22] J. Li, S. Liu, H. Zhou, L. Qu, J. Yang, starBase v2.0: decoding miRNA-ceRNA, miRNA-ncRNA and protein-RNA interaction networks from large-scale CLIP-Seq data, Nucleic Acids Res. 42 (Database issue) (2014) D92–D97, https://doi.org/10.1093/nar/gkt1248.

[23] N. Zhou, J. Bao, FerrDb: a Manually Curated Resource for Regulators and Markers of Ferroptosis and Ferroptosis-Disease Associations, Database, Oxford, 2020, p. 2020, https://doi.org/10.1093/database/baaa021.

[24] D. Bu, H. Luo, P. Huo, Z. Wang, S. Zhang, Z. He, Y. Wu, L. Zhao, J. Liu, J. Guo, et al., KOBAS-i: intelligent prioritization and exploratory visualization of biological functions for gene enrichment analysis, Nucleic Acids Res. 49 (W1) (2021) W317–W325, https://doi.org/10.1093/nar/gkab447.

[25] D. Szklarczyk, A.L. Gable, K.C. Nastou, D. Lyon, R. Kirsch, S. Pyysalo, N.T. Doncheva, M. Legeay, T. Fang, P. Bork, et al., The STRING database in 2021: customizable protein-protein networks, and functional characterization of user-uploaded gene/measurement sets, Nucleic Acids Res. 49 (D1) (2021) D605–D612, https://doi.org/10.1093/nar/gkaa1074.

[26] P. Shannon, A. Markiel, O. Ozier, N.S. Baliga, J.T. Wang, D. Ramage, N. Amin, B. Schwikowski, T. Ideker, Cytoscape: a software environment for integrated models of biomolecular interaction networks, Genome Res. 13 (11) (2003) 2498–2504.

[27] C. Chin, S. Chen, H. Wu, C. Ho, M. Ko, C. Lin, cytoHubba: identifying hub objects and sub-networks from complex interactome, BMC Syst. Biol. 8 (Suppl 4) (2014) S11, https://doi.org/10.1186/1752-0509-8-S4-S11. Suppl 4.

[28] Y. Li, C. Huang, Z. Yang, L. Wang, D. Luo, L. Qi, Z. Li, Y. Huang, Identification of potential biomarkers of gout through competitive endogenous RNA network analysis, Eur. J. Pharmaceut. Sci. 173 (2022), 106180, https://doi.org/10.1016/j.ejps.2022.106180.

[29] S. Ghafouri-Fard, A. Abak, H. Shoorei, M. Mohaqiq, J. Majidpoor, A. Sayad, M. Taheri, Regulatory role of microRNAs on PTEN signaling, Biomed. Pharmacother. 133 (2021), 110986, https://doi.org/10.1016/j.biopha.2020.110986.

[30] R. Yin, J. Jiang, H. Deng, Z. Wang, R. Gu, F. Wang, miR-140-3p aggregates osteoporosis by targeting PTEN and activating PTEN/PI3K/AKT signaling pathway, Hum. Cell 33 (3) (2020) 569–581, https://doi.org/10.1007/s13577-020-00352-8.

[31] E.G. Ramírez-Salazar, S. Carrillo-Patiño, A. Hidalgo-Bravo, B. Rivera-Paredez, M. Quiterio, P. Ramírez-Palacios, N. Patiño, M. Valdés-Flores, J. Salmerón, R. Velázquez-Cruz, Serum miRNAs miR-140-3p and miR-23b-3p as potential biomarkers for osteoporosis and osteoporotic fracture in postmenopausal Mexican-Mestizo women, Gene 679 (2018) 19–27, https://doi.org/10.1016/j.gene.2018.08.074.

[32] J. Chai, L. Xu, N. Liu, miR-23b-3p regulates differentiation of osteoclasts by targeting PTEN via the PI3k/AKT pathway, Arch. Med. Sci. 18 (6) (2022) 1542–1557, https://doi.org/10.5114/aoms.2019.87520.

[33] J. Li, X. Chen, L. Lu, X. Yu, The relationship between bone marrow adipose tissue and bone metabolism in postmenopausal osteoporosis, Cytokine Growth Factor Rev. 52 (2020) 88–98, https://doi.org/10.1016/j.cytogfr.2020.02.003.

[34] Y. Liu, Y. He, B. He, L. Kong, The anti-osteoporosis effects of vitamin K in postmenopausal women, Curr. Stem Cell Res. Ther. 17 (2) (2022) 186–192, https://doi.org/10.2174/1574888X16666210512020103.

[35] C. Chen, J. Chen, L. He, B.L. Stiles, PTEN: tumor suppressor and metabolic regulator, Front. Endocrinol. 9 (2018) 338, https://doi.org/10.3389/fendo.2018.00338.

[36] W. Zhang, S. Cui, H. Yi, X. Zhu, W. Liu, Y. Xu, MiR-708 inhibits MC3T3-E1 cells against H2O2-induced apoptosis through targeting PTEN, J. Orthop. Surg. 15 (1) (2020) 255, https://doi.org/10.1186/s13018-020-01780-w.

[37] L. Yang, Y. Li, R. Gong, M. Gao, C. Feng, T. Liu, Y. Sun, M. Jin, D. Wang, Y. Yuan, et al., The long non-coding RNA-ORLNC1 regulates bone mass by directing mesenchymal stem cell fate, Mol. Ther. 27 (2) (2019) 394–410, https://doi.org/10.1016/j.ymthe.2018.11.019.

[38] Y. Chen, F. Zhou, H. Liu, J. Li, H. Che, J. Shen, E. Luo, SIRT1, a promising regulator of bone homeostasis, Life Sci. 269 (2021), 119041, https://doi.org/10.1016/j.lfs.2021.119041.

[39] X. Yang, T. Jiang, Y. Wang, L. Guo, The role and mechanism of SIRT1 in resveratrol-regulated osteoblast autophagy in osteoporosis rats, Sci. Rep. 9 (1) (2019), 18424, https://doi.org/10.1038/s41598-019-44766-3.

[40] C. Jin, K. Tan, Z. Yao, B. Lin, D.-P. Zhang, W. Chen, S. Mao, W. Zhang, L. Chen, Z. Lin, et al., A novel anti-osteoporosis mechanism of VK2: interfering with ferroptosis via AMPK/SIRT1 pathway in type 2 diabetic osteoporosis, J. Agric. Food Chem. 71 (6) (2023) 2745–2761, https://doi.org/10.1021/acs.jafc.2c05632.

[41] T. Yu, X. You, H. Zhou, W. He, Z. Li, B. Li, J. Xia, H. Zhu, Y. Zhao, G. Yu, et al., MiR-16-5p regulates postmenopausal osteoporosis by directly targeting VEGFA, Aging 12 (10) (2020) 9500–9514, https://doi.org/10.18632/aging.103223.

[42] Z. Wang, X. Ge, Y. Wang, Y. Liang, H. Shi, T. Zhao, Mechanism of dexmedetomidine regulating osteogenesis-angiogenesis coupling through the miR-361-5p/VEGFA axis in postmenopausal osteoporosis, Life Sci. 275 (2021), 119273, https://doi.org/10.1016/j.lfs.2021.119273.

[43] W. Wu, Q. Li, Y. Liu, Y. Li, lncRNA GAS5 regulates angiogenesis by targeting miR-10a-3p/VEGFA in osteoporosis, Mol. Med. Rep. 24 (4) (2021), https://doi.org/10.3892/mmr.2021.12350.

[44] J. Chen, C. Yan, H. Yu, S. Zhen, Q. Yuan, miR-548d-3p inhibits osteosarcoma by downregulating KRAS, Aging 11 (14) (2019) 5058–5069, https://doi.org/10.18632/aging.102097.

[45] M.R. Zinatizadeh, S.A. Momeni, P.K. Zarandi, G.M. Chalbatani, H. Dana, H.R. Mirzaei, M.E. Akbari, S.R. Miri, The role and function of ras-association domain family in cancer: a review, Genes Dis 6 (4) (2019) 378–384, https://doi.org/10.1016/j.gendis.2019.07.008.

[46] M. Hu, X. Zhu, H. Yuan, H. Li, H. Liao, S. Chen, The function and mechanism of the miR-210-3p/KRAS axis in bone marrow-derived mesenchymal stem cell from patients with osteoporosis, J Tissue Eng Regen Med 15 (8) (2021) 699–711, https://doi.org/10.1002/term.3215.
[47] A. Gallardo, E. Lerma, D. Escuin, A. Tibau, J. Muñoz, B. Ojeda, A. Barnadas, E. Adrover, L. Sánchez-Tejada, D. Giner, et al., Increased signalling of EGFR and IGF1R, and deregulation of PTEN/PI3K/Akt pathway are related with trastuzumab resistance in HER2 breast carcinomas, Br. J. Cancer 106 (8) (2012) 1367–1373, https://doi.org/10.1038/bjc.2012.85.
[48] J. Yi, J. Zhu, J. Wu, C.B. Thompson, X. Jiang, Oncogenic activation of PI3K-AKT-mTOR signaling suppresses ferroptosis via SREBP-mediated lipogenesis, Proc. Natl. Acad. Sci. U. S. A. 117 (49) (2020) 31189–31197, https://doi.org/10.1073/pnas.2017152117.
[49] J. Hao, J. Bei, Z. Li, M. Han, B. Ma, P. Ma, X. Zhou, Qing'e Pill Inhibits Osteoblast Ferroptosis via ATM Serine/Threonine Kinase (ATM) and the PI3K/AKT Pathway in Primary Osteoporosis, Front. Pharmacol. 13 (2022), 902102, https://doi.org/10.3389/fphar.2022.902102.